CO_2 activation on TiO_2-supported Cu_5 and Ni_5 nanoclusters : effect of plasma-induced surface charging

THE JOURNAL OF PHYSICAL CHEMISTRY C

MACQUARIE University SYDNEY·AUSTRALIA

Subscriber access provided by Macquarie University

C: Surfaces, Interfaces, Porous Materials, and Catalysis

CO Activation on TiO-Supported Cu and Ni Nanoclusters: Effect of Plasma-Induced Surface Charging

Amin Jafarzadeh, Kristof M. Bal, Annemie Bogaerts, and Erik Cornelis Neyts

J. Phys. Chem. C, **Just Accepted Manuscript** • DOI: 10.1021/acs.jpcc.8b11816 • Publication Date (Web): 21 Feb 2019

ACS Publications

is published by the American Chemical Society. 1155 Sixteenth Street N.W., Washington, DC 20036

CO_2 Activation on TiO_2-supported Cu_5 and Ni_5 Nanoclusters: Effect of Plasma-Induced Surface Charging

A. Jafarzadeh*, K. M. Bal, A. Bogaerts and E. C. Neyts

Research group PLASMANT, Department of Chemistry, University of Antwerp, Universiteitsplein 1, 2610 Wilrijk-Antwerp, Belgium

Abstract

Surface charging is an often overlooked factor in many plasma-surface interactions and in particular in plasma catalysis. In this study, we investigate the effect of excess electrons induced by a plasma on the adsorption properties of CO_2 on titania-supported Cu_5 and Ni_5 clusters using spin polarized and dispersion corrected density functional theory (DFT) calculations. The effect of excess electrons on the adsorption of Ni and Cu pentamers as well as on CO_2 adsorption on a pristine anatase TiO_2 (101) slab is studied. Our results indicate that adding plasma-induced excess electrons to the system leads to a further stabilization of the bent CO_2 structure. Also dissociation of CO_2 on the charged clusters is energetically more favorable than on the neutral clusters. We hypothesize that surface charge is a plausible cause for the synergistic effects sometimes observed in plasma catalysis.

Introduction

Plasma catalysis[1, 2] holds promise for many environmental[3-8] and industrial [9, 10] applications. Combining a plasma with a catalyst induces a complex reciprocal interaction, which in some cases leads to synergistic effects that improve the efficiency of the catalytic reactions. However, the underlying reasons for synergy in plasma catalysis remain unknown. Reaction promotion in catalytic removal of NO_x,[11] higher CO_2 conversion,[12] decrease in energy barrier for dry reforming of methane (DRM)[13] and increased treatment efficiency on Escherichia coli cells in aqueous media[14] have been reported as a result of synergistic effects in plasma catalysis.

Plasma is an ionized gas that consists of different interacting species such as electrons, ions, neutral atoms, and vibrationally and electronically excited species. The presence of these species makes the plasma a highly reactive but non-selective environment that is very suitable for combining with a catalyst.[2] In particular, the plasma leads to a modification of the gas phase (and hence the reactants), while still allowing for a (relatively) low temperature. The contribution of all the specific plasma factors strongly depends on the type of plasma and the working conditions, and has been studied extensively. The mechanisms of plasma-induced changes in the catalyst structural and electronic properties remain largely unresolved. In order to unravel (some of) the mechanisms underlying plasma-catalyst interactions we need to narrow down the complexity of the system by focusing on a specific factor and its effect on the whole plasma-catalytic process. Complementary to experiments, computer simulations are ideally suited for this.

A catalyst surface becomes inevitably charged upon interaction with plasma. The accumulated surface charge can alter the catalyst electronic and geometric structures, consequently leading to a change in the kinetics of the whole catalytic reaction. Even changes in activity of the different geometric structures of a catalyst are generally ascribed to differences in their electronic

structures.[15] Hence, by considering electronic properties of the catalyst during its interaction with plasma, one can gain information about the effect of plasma-induced surface charging on catalytic reactions.

The effect of surface charging, for instance due to plasma, is important in heterogeneous catalysis and in particular when transition metal clusters are deposited on oxide surfaces. Excess electrons accumulated on the oxide surface can alter the electronic structure and adsorption properties of the supported transition metal nanoparticles. Although there have been experimental[16, 17] and theoretical[18, 19] investigations on the effect of plasma in heterogeneous catalysis, and studies have been carried out on the deposition of metal clusters on oxide surfaces without plasma,[20-22] the effect of plasma-induced excess electrons on the deposition of metal clusters and their catalytic properties has been scarcely investigated. Both nickel and copper are widely used in heterogeneous catalysis, for instance, for CO_2 conversion [18, 23, 24] e.g. for forming value-added products like methanol. We here choose to study Ni and Cu pentamers. First, these clusters can be synthesized and are actually used in the catalysis community. Further, because of their small size, they require less material, making them cheaper (per unit surface area) and possibly more environmentally friendly. Finally, considering the limited number of possible isomers, their fluxionality (in gas phase) is much less than larger clusters, which makes them computationally tractable.

In this study we report on the role of excess electrons on (1) the adsorption of Ni_5 and Cu_5 clusters on an anatase TiO_2 (101) slab as test systems; (2) adsorption of an adsorbate molecule (CO_2) on the stoichiometric surface of anatase TiO_2 (101); (3) adsorption of a CO_2 molecule on TiO_2-supported Ni_5 and Cu_5 clusters; and (4) dissociation of the CO_2 molecule.

As a reducible oxide, TiO_2 is an interesting candidate to investigate the effects of surface charging. Among the various polymorphs of titania, anatase has been widely used in modeling catalytic reactions.[20-22, 25, 26] The (101) plane of anatase (a-TiO_2) has been chosen for the adsorption of the metal clusters because of its high thermodynamic stability.[21]

Computational details

All calculations have been carried out based on spin polarized density functional theory (DFT) by using the Quickstep [27] module of the CP2K[28] package. This module mainly employs localized Gaussian orbitals and auxiliary plane waves as a dual basis for expanding the Kohn-Sham orbitals. Double–ζ valence plus polarization (DZVP) basis sets which are optimized from molecular interactions (MOLOPT)[29] combined with a plane wave basis set with 800 Ry cutoff have been used for the calculations. Goedecker-Teter-Hutter (GTH) pseudopotentials[30, 31] are used for describing the inner shell electrons; for C, O, Cu, Ti and Ni atoms, 4, 6, 11, 12 and 18 valence electrons are explicitly considered, respectively. The general gradient approximation (GGA) Perdew-Burke-Ernzerhof (PBE)[32] functional is applied for treating electron exchange and correlation effects. Dispersion interactions are included through Grimme's D3 approximation along with Becke-Jonsson damping.[33, 34] The Broyden-Fletcher-Goldfarb-Shanno (BFGS) scheme is used for geometry optimization where a maximum force of 0.02 eV/Å has been set for the relaxation of atoms. k-point sampling is limited to the Γ–point only and the Hirshfeld-I scheme[35] is used for charge analysis of interactions between the adsorbates and the slab surface.

Lattice parameters of bulk anatase TiO_2 ($a = b = 3.7845$ Å and $c = 9.5143$ Å)[36] were used for creating the surface slabs. A slab of anatase (101) with dimensions of 10.239 × 11.3535 × 30.00 $Å^3$ (1 × 3 supercell) consisting of 6 (O-Ti-O) trilayers and containing 108 atoms (Fig. 1) was used

for the calculations. To mimic the bulk-like structure we fixed the bottom layers of the support in a first set of calculations. This, however, also leads to interference in the excess electron's localization pattern. Thus, we also examined a fully relaxed structure, with no atoms frozen. The results with the fixed layers are mainly provided in the supporting information (SI); we here mainly focus on the results achieved without applying any constraint on relaxation of the atoms. Calculations for the metal clusters and the CO_2 molecule in gas phase have been done in a box of $15 \times 15 \times 15$ Å^3 dimensions.

For the treatment of charged configurations, we applied our recently proposed method[37] suitable for modeling plasma-surface interactions. In this approach, we use a positive countercharge located far from the surface (in the z-direction) without assigning a local basis set to it. Thus, the electron density is not allowed to be distributed around the ion but rather it will be localized on the surface. This is an ideal approach for modeling the effect of plasma-induced excess electrons on the surface of a catalyst, because it explicitly incorporates both the negative charging from excess electrons, as well as polarization effects and electric fields arising from positively charged ions in the plasma sheath region in the gas phase.

Electrostatic interactions were described with the Martyna-Tuckerman (MT) Poisson solver[38], which requires the z-component of the cell size to be very large (100 Å) for charged configurations. The MT solver allows to impose full periodicity along the surface slab (in the xy plane), mimicking a semi-infinite catalyst surface, while simultaneously removing periodicity along the z direction. As such, unphysical interactions of the slab with itself are avoided, which would otherwise result in significant computational artefacts when dealing with charged surfaces[39].

We employed DFT+U[40, 41] calculations for cross-checking the results, while accounting for the strong on-site Coulomb interactions. By using this approach, the self-interaction effect for Ti d-

orbitals will be corrected by Hubbard's U parameter. This parameter is set to 5 eV for Ti atoms. Considering the small number of atoms in clusters studied in this work, and negligible impact of their self-interaction on the results, no Hubbard parameter is applied to the d-orbitals of Ni and Cu atoms. Considering that DFT+U provides a better picture for electron localization on support cations, we have referred to the PDOS and spin density diagrams obtained by the DFT+U calculations.

We have investigated the effect of charge in two ways: First, re-optimization of the neutral structure after adding an excess electron to the system, and second, optimization of the initially negatively charged configuration. After finding the most stable mode for both neutral and charged configurations, we have made a comparison between the corresponding adsorption energies and other properties for the neutral and negatively charged structures.

Adsorption energies of clusters on anatase are calculated based on equation (1), where $E_{cluster}$ is the total energy of the Ni_5/Cu_5 clusters, $E_{slab+cluster}$ is the total energy of the complex (consisting of cluster and surface) and E_{slab} is the total energy of the bare slab:

$$E_{Adsorption} = E_{slab+cluster} - E_{cluster} - E_{slab} \quad (1)$$

Similarly, the adsorption energy of CO_2 on the supported cluster is calculated as:

$$E_{Adsorption} = E_{complex+molecule} - E_{complex} - E_{molecule} \quad (2)$$

Thermal and zero-point energy calculations are not considered.

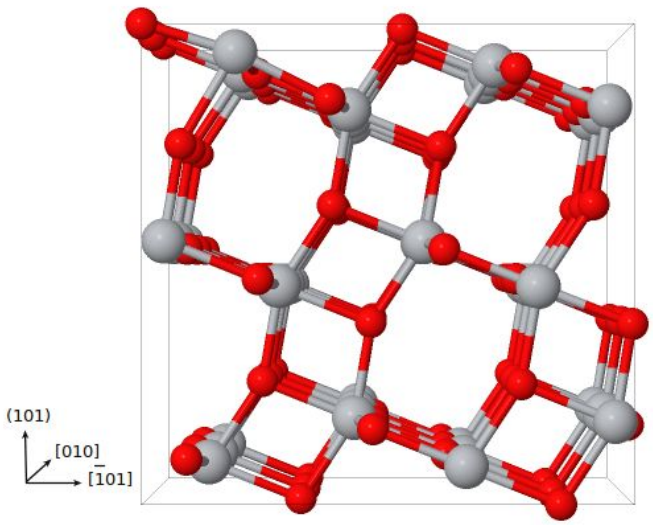

Figure 1: (1 × 3) supercell of anatase TiO_2 (101)

Results and discussion

Adsorption of Ni_5 and Cu_5 clusters on the anatase (101) surface

To investigate the adsorption of Cu_5 and Ni_5 on the TiO_2 surface, we first optimized their structure in the gas phase, as described in the SI. Then, the clusters were deposited on the neutral anatase (101) surface and their adsorption energy was calculated. Subsequently, one electron was added to this configuration, and the system was re-optimized. This allowed us to compare the adsorption properties of each metal cluster in the neutral and charged systems. Similar to the gas phase calculations, we explored 5 initial structures with different orientations of the cluster adsorbing on the surface. Then we examined the most stable orientation in 5 different adsorption sites. The most stable configurations found for the adsorption of Ni_5 and Cu_5 clusters are shown in Fig. 2 while the unstable adsorption modes are provided in the SI. We acknowledge that this procedure does not guarantee finding the global minimum.

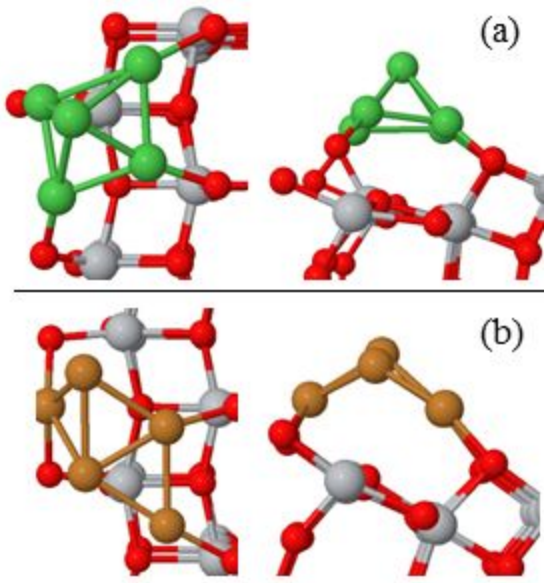

Figure 2: Top and side view of the most stable configurations of (a) Ni_5 and (b) Cu_5 clusters on anatase TiO_2 (101) slab

Upon adsorption, hardly any change in shape of the Ni_5 cluster is seen. Adsorption of the Ni_5 cluster on the anatase surface changes the electronic structure of the support such that the Ni d-orbitals fill the band-gap of the TiO_2 semiconductor (see the SI) in agreement with literature.[42, 43] Population analysis based on the Hirshfeld scheme shows that during the adsorption of Ni_5 there is a charge transfer from the support to the cluster. For the gas phase Ni_5 cluster, the total spin moment $(n_\alpha - n_\beta)$ is $2\,\mu_B$ (triplet state) which changes to $3.1\,\mu_B$ upon adsorption. Also the accumulated net charge of $-0.893\ |e|$ on the Ni_5 cluster shows that there is a significant charge transfer between the cluster and the surface which leads to a high adsorption energy of -5.72 eV. This electron transfer from the support to the cluster leaves the support with one unpaired electron as can be seen from the spin density isosurfaces (Fig. 3a).

Upon adsorption, the Cu_5 cluster changes its original planar configuration to a more 3D structure facilitating strong interaction between the cluster and the oxide surface with an adsorption energy

of -4.29 eV. In comparison to Ni_5, the d-orbitals of the Cu_5 cluster partially lie in the TiO_2 band gap with a tendency to be located near the valence band (see the SI). Charge transfer direction between the support and cluster is different for Ni_5 and Cu_5. The Cu_5 has a total spin moment of 2 μ_B (doublet state) in the gas phase which changes to 0 after its adsorption on the support surface. During the adsorption, one unpaired electron in the Cu_5 cluster is transferred to the support. From Fig. 3(c) we can see that the transferred electron localizes on the subsurface Ti atom of the support.

After adding an excess electron to the relaxed neutral structures and re-optimization, no change in the adsorption mode is seen. Changes in adsorption energies as described below can therefore (mostly) be attributed to the effect of the negative charge (Fig. 4). Adding a single excess electron to the surface model leads to an electron density of $8.6 \times 10^{17} m^{-2}$ or a surface charge density of $-0.137 \frac{C}{m^2}$, which is in the same order of experimental estimates of plasma-deposited charge densities on dielectrics,[44] and a factor of four higher than reported in recent particle-in-cell/Monte Carlo collision PIC/MCC simulations for plasma in contact with dielectric surfaces or catalyst pores[45].

From the spin density analysis (Fig. 3b) we can see that for the charged Ni_5 structure, the added electron is mostly localized on the Ni cluster, changing its net charge to -1.643 |e| and also the total net spin moment to $2.2\mu_B$. This gives rise to a change in adsorption energy of the cluster by $+0.06$ eV, amounting to an adsorption energy of -5.66 eV. However, in Fig. 4, the DFT result without U correction shows that upon charging, the adsorption energy decreases by -0.51 eV, which is mostly because of the failure in localization of the excess electron.

In contrast, upon negatively charging the surface, no spin polarization on the Cu_5 is seen, which means that the added electron is not localized on the cluster (i.e., the net spin moment of the cluster remains zero). Instead, as can be seen from Fig. 3d, the presence of excess electrons leads to a

change in the localization of the previously transferred electron. Eventually, two electrons are localized on the surface of the support, which decreases the adsorption energy by 1.20 eV for the Cu_5 cluster, amounting to an adsorption energy of -5.49 eV. A detailed summary of the changes in net spin moment and partial charges of the atoms for both neutral and charged structures is provided in the SI.

These results highlight the different effect of excess charge on the adsorption properties of Cu and Ni pentamers. Methodologically, these results also show that depending on the localization procedure of the excess electron, its effect on stabilization of the adsorbed metal clusters can be different. Furthermore, it is seen that for fully relaxed systems, DFT calculations without considering on site Coulomb interactions have difficulties describing the effect of excess electrons on the stability of the metal clusters.

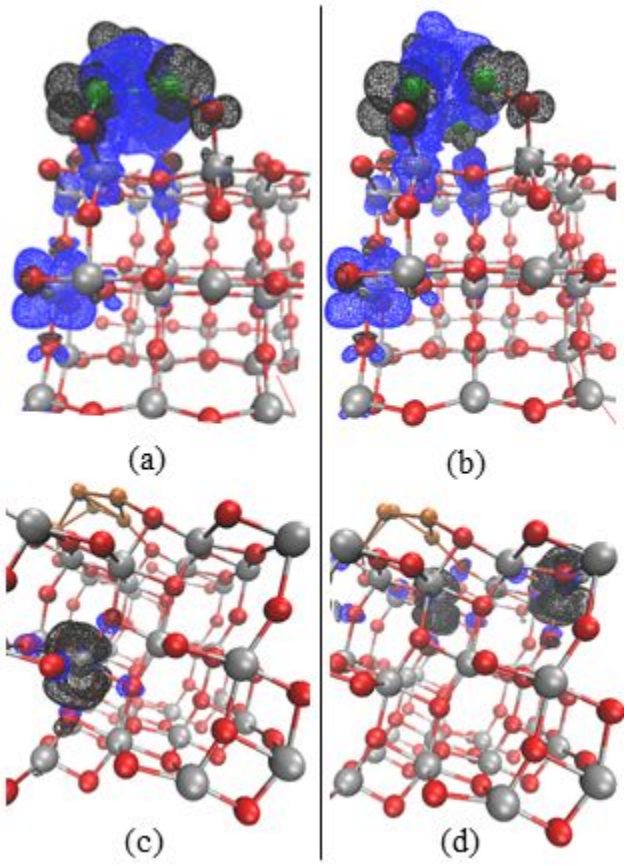

Figure 3: Spin density isosurfaces for a) neutral Ni_5/TiO_2, b) charged Ni_5/TiO_2, c) neutral Cu_5/TiO_2 and d) charged Cu_5/TiO_2 structures. The black and blue lobes correspond to spin up and spin down, respectively. Isovalues are set to $\pm$ 0.001 e/Å^3

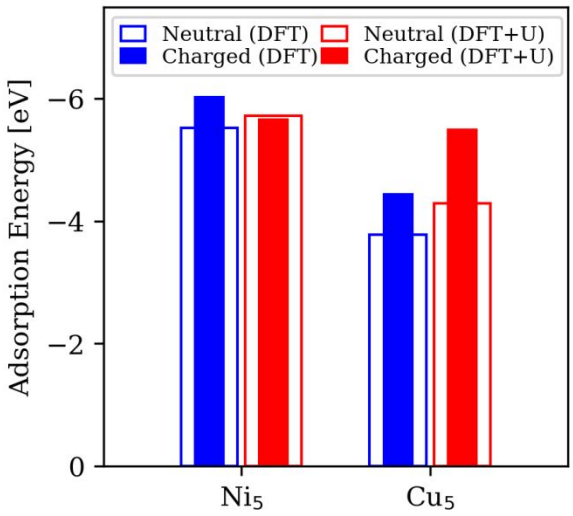

Figure 4: Adsorption energies of Ni_5 and Cu_5 clusters on anatase TiO_2 (101)

CO_2 adsorption on anatase TiO_2 (101)

CO_2 adsorption on neutral anatase was previously studied by DFT.[43, 44, 46] In this study our aim is to investigate the effect of plasma-induced excess electrons on the adsorption of CO_2 on both the bare surface and on titania-supported Ni_5 and Cu_5 clusters. We will focus on the two most stable configurations for the adsorption of CO_2 on the anatase (101) surface, shown in Fig. 5.

We first kept the three layers of the TiO_2 slab frozen in their bulk structure to allow for a direct comparison between the results for neutral structures and the literature. For the linear configuration, we find that CO_2 adsorbs on the neutral surface with an adsorption energy of -0.44 eV and -0.51 eV for DFT and DFT+U, respectively. The bent structure shows an adsorption energy of -0.03 eV using DFT, while DFT+U yields an adsorption energy of -0.18 eV. It can be seen that the results coming from DFT+U are in agreement with the values of -0.48 eV for linear and -0.16 eV for carbonate-like structure, as reported by Sorescu et al.[44] Iyemperumal et al[43] reported values of -0.40 eV and -0.09 eV for the most stable linear and bent structures,

respectively. Results for both neutral and charged structures of CO_2 adsorption on bare TiO_2 (with fixed bottom layers) are shown in Fig. 6a.

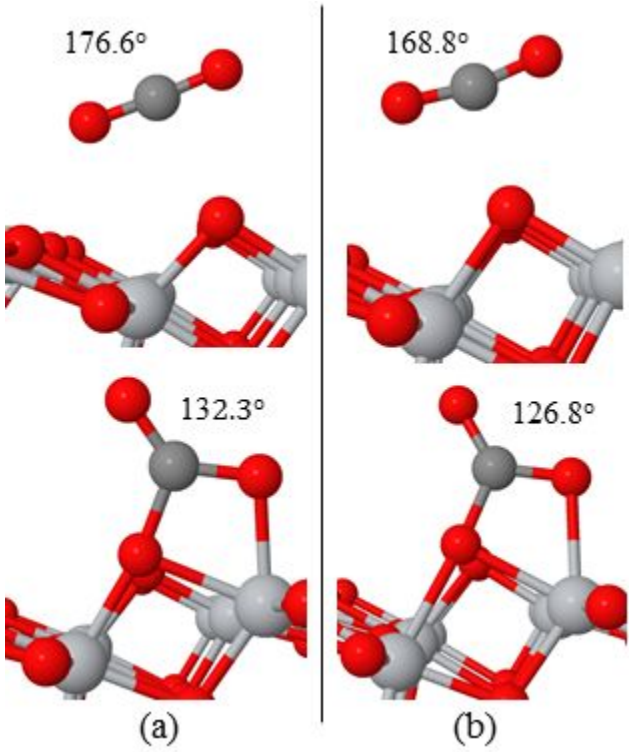

Figure 5: The most stable configurations for the linear and bent CO_2 structures adsorbing on TiO_2 (101) surface. a) neutral and b) charged configurations

By removing the constraint on the bottom layers of the slab, the electron distribution is unbiased, which permits a reliable comparison between the neutral and charged structures. The results for fully relaxed systems are provided in Fig. 6b. As we can see from this figure, the trends are maintained, although there are quantitative differences in adsorption energies achieved for the system with fixed layers.

By adding charge to the system, both adsorption modes essentially maintain their structure. In the linear adsorption mode, the effect of excess charge on the adsorption energy is less pronounced. In this case, there is no mixing between the states of the molecule and the surface, such that the (small) increase in adsorption energy of the linear CO_2 can be attributed to polarization effects. In

this case electrostatic Coulomb forces between the positive C atom and the negatively charged surface will lead to an improvement in adsorption energy. The PDOS of the linear adsorption mode for both neutral and charged structures (Fig. 7a,7b) reveals that upon charging, the states of both oxygen atoms of the CO_2 molecule are shifted toward lower energies and this leads to a small improvement in stabilization of the molecule.

For the bent structure there is a substantial increase in adsorption energy upon charging, to -1.13 eV and -1.40 eV in DFT and DFT+U, respectively, which is also reflected in the partial charges of CO_2 in the neutral and charged configurations: the partial charges on oxygen atoms of CO_2 molecule change from $-0.862\,|e|$ and $-0.624\,|e|$ (neutral system) to $-1.028\,|e|$ and $-0.728\,|e|$ (charged system). Considering that the surface Ti atom bonded to the oxygen atom of the CO_2 molecule has preserved its net charge from the neutral configuration, we can see that the increase in adsorption energy is mainly due to the change in partial charge of the molecule. This is consistent with the PDOS diagrams (Fig. 7d) of the charged configuration, showing a shift in the DOS of the oxygen atoms of CO_2 towards the valence band, facilitating the pronounced mixing with orbitals of the surface Ti atoms, in comparison to the neutral case.

Table 1 shows the effect of charge on the adsorption energy of the two most stable modes of CO_2 on titania achieved by DFT and DFT+U. The same trend is clear from the results shown in Fig. 6.

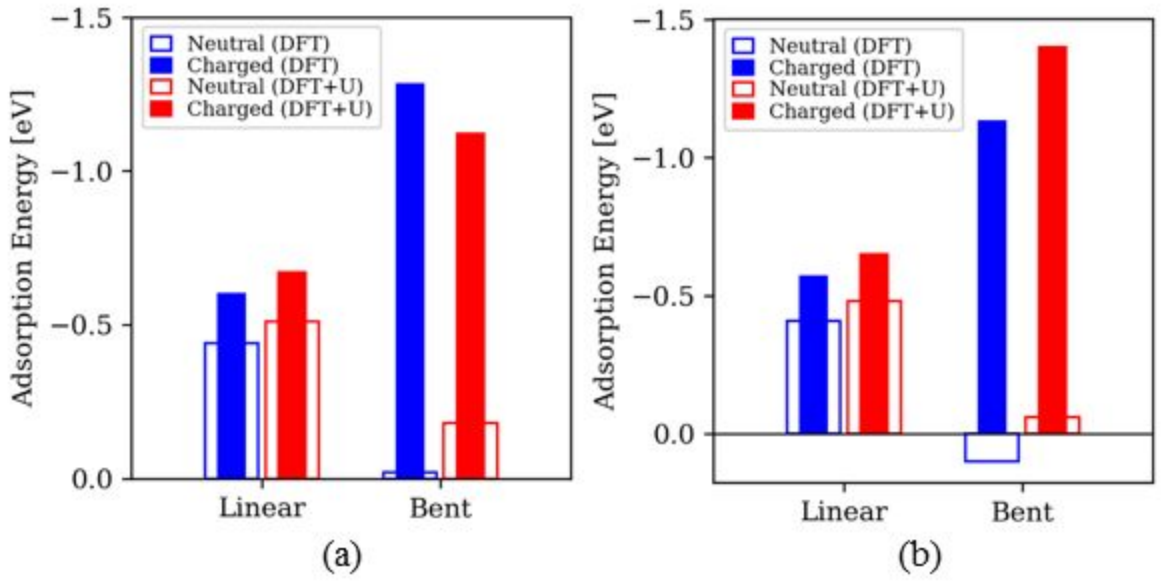

Figure 6: CO_2 adsorption energy for both linear and bent structures on neutral and charged configurations of anatase (101) - a) structures with 3 bottom layers kept frozen and b) fully relaxed structures

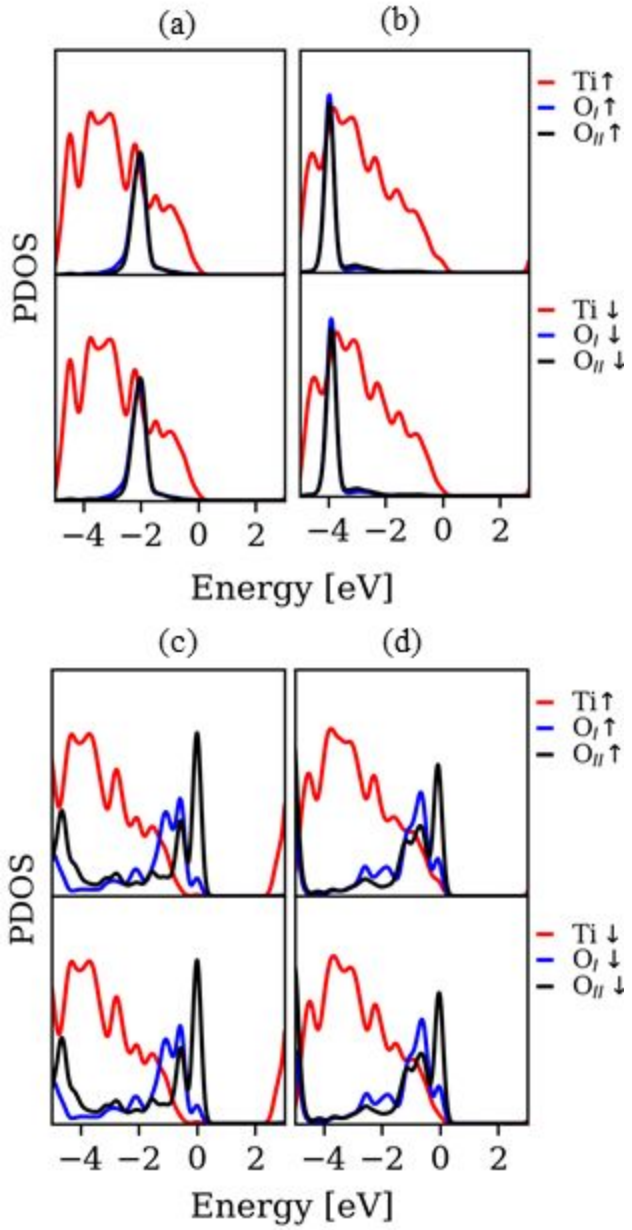

Figure 7: Projected density of states for the adsorption of a CO_2 molecule on TiO_2. a) linear-neutral, b) linear-charged c) bent-neutral and d) bent-charged structures. O_I and O_{II} are oxygen atoms of the CO_2 molecule. Up/down spin states are shown with up/down arrows.

Transformation of the linear to the bent structure thus seems essential for CO_2 activation. It is clear from the results that adding a plasma–deposited excess electron to the system changes the most stable structure of the CO_2 adsorbed on titania surface from a linear to a bent configuration,

which makes the activation of the CO_2 molecule thermodynamically more favorable. Correspondingly, we also analyzed changes in C-O bond length and in O-C-O bond angle, as a result of negatively charging the surface. In Table 1, we summarize the results for the effect of charge on bond lengths and angles. It can be seen that the presence of excess charge has impact on bending the CO_2 molecule, while the effect on C-O bond elongation is limited.

Table 1: Bond lengths and adsorption energies of CO_2 with both linear and bent structures in neutral and charged configurations

Method	Structure	r(C-O)	α (OCO)	E_{ads} (eV)
DFT	Gas Phase	1.17, 1.17	180	
	Bent (Neutral)	1.20, 1.32	131.6	0.10
	Bent (Charged)	1.23, 1.32	126.4	-1.13
	Linear (Neutral)	1.17, 1.18	177.2	-0.41
	Linear (Charged)	1.18, 1.18	169.9	-0.57
DFT+U	Bent (Neutral)	1.20, 1.32	132.3	-0.06
	Bent (Charged)	1.23, 1.32	126.8	-1.40
	Linear (Neutral)	1.17, 1.18	176.6	-0.48
	Linear (Charged)	1.18, 1.18	168.8	-0.65

CO_2 adsorption on supported clusters

For the adsorption of CO_2 on titania-supported clusters, various initial modes were examined. In this case, we optimized each initial structure both with and without the presence of plasma-induced excess electrons.

Adsorption of CO_2 on the supported Ni_5 cluster does not lead to a marked change in shape of the cluster. Bond formation between the CO_2 molecule and Ni atoms of the cluster results in a bent structure of CO_2 (Fig. 8a) with an adsorption energy of -0.53 and -031 eV for DFT and DFT+U, respectively. During CO_2 adsorption, the net spin moment of the cluster remains at 3 μ_B, while its net charge increases from -0.893 |e| to -1.412 |e|, indicating the formation of a polar covalent bond between the cluster and the C atom of the CO_2 molecule. The Ni atom which bonds to C has a net charge of -0.730 |e|, while the carbon atom has a charge of 1.769 |e|.

Adsorption of CO_2 on the supported Cu_5 cluster results in a noticeable change in the cluster shape. In this case, CO_2 adsorbs on the interface via the C atom making bonds with two copper atoms of the cluster and the oxygen atom with a surface Ti atom (Fig. 8c). In this configuration, the Cu_5 cluster has three coordinations with surface oxygens and three with the CO_2 molecule, while maintaining a net spin moment of 0 and having partial net charge of -0.205 |e|. The net charge for the carbon and the two Cu atoms of the cluster is 1.502 |e|, -0.064 |e| and -0.228 |e|, respectively. This shows the formation of a covalent bond between the cluster and the CO_2 molecule.

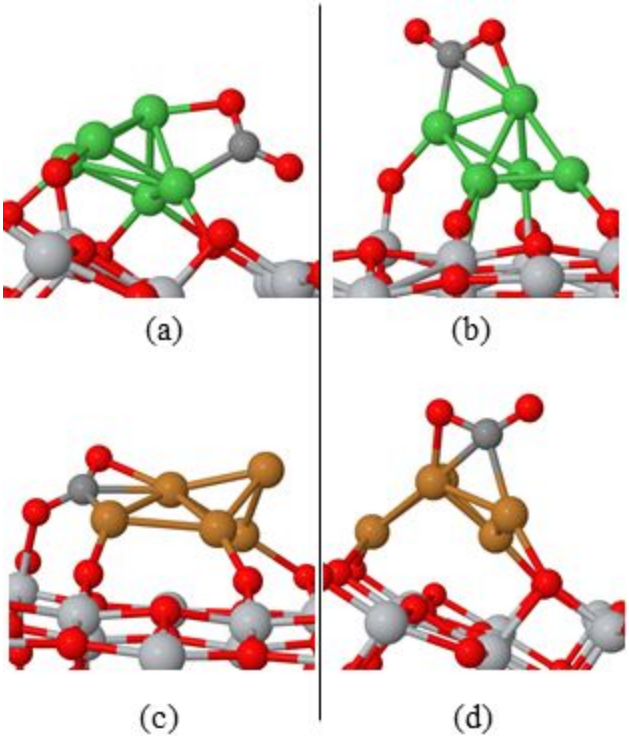

Figure 8: Adsorption of CO_2 on supported a) Ni_5 - neutral, b) Ni_5 - charged, c) Cu_5 - neutral and d) Cu_5 - charged structures

Bond lengths and adsorption energies of CO_2 on Ni_5 and Cu_5 clusters supported by anatase TiO_2 (101) are shown in Table 2. From this table and also from Fig. 9, we observe a noticeable improvement in stability of the CO_2 molecule adsorbed on both clusters upon negatively charging the surface.

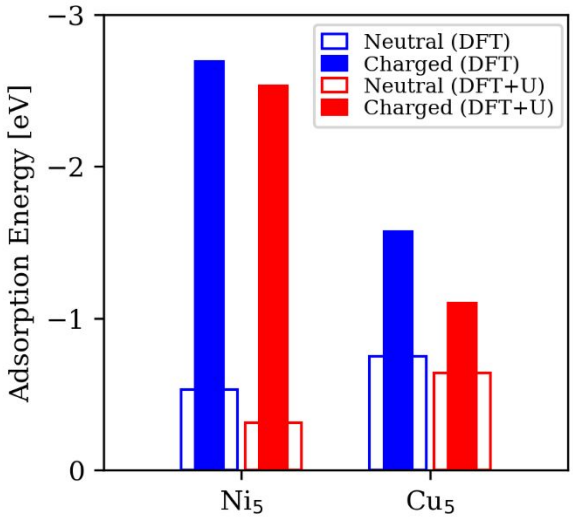

Figure 9: Adsorption energy of CO_2 molecule on Ni_5/Cu_5 clusters supported by anatase TiO_2 (101)

The increase in adsorption energy in case of the charged Ni_5 structure is mostly because of the extra bond formation between the C atom and the top Ni atom of the cluster (Fig. 8b). Together with a net spin moment of 2 μ_B, the net charge on the cluster increases to –1.708 |e|, explaining the stronger bond between the cluster and the (positively charged) C atom of the molecule. The PDOS reveals that upon charging there is a shift in bonding states of the CO_2 molecule towards the valence band (Fig. 10b). This leads to facilitation of the hybridization of high-lying CO_2 antibonding π^* orbitals with *d* orbitals of the cluster. This shift is also seen in CO_2 adsorption on a negatively charged slab of titania, which resulted in improved adsorption energy of the carbonate-like structure.

For the CO_2 adsorption on the negatively charged Cu_5/TiO_2 (Fig. 8d), we can see a slightly smaller bandgap (Fig. 10d), together with higher hybridization of C states with the cluster d orbitals. By analyzing the spin population and net charge of each atom, together with the morphological changes in the cluster shape upon charging the system, we can see that for the charged configuration, the CO_2 molecule binds only with the metal cluster, in contrast to the

neutral case, in which CO_2 binds to the interface. This change in adsorption mode is accompanied by a change in the amount of accumulated charge on the CO_2 molecule (from +0.184 |e| to –0.268 |e| upon negatively charging the system). The net spin moment remains zero, while the net charge on the cluster increases as a result of the presence of the excess electron. Considering the unpolarized spin configuration of the cluster, we conclude that the net charge of the cluster is actually the amount of charge that it shares with the surface as a result of their interaction. Thus, the improved adsorption energy of the CO_2 molecule on negatively charged Cu_5/TiO_2 is actually due to more hybridization of the CO_2 states with cluster's orbitals and also stronger interaction of the complex of cluster + molecule with support's surface (considering that the amount of charge shared between the cluster and the support has been increased).

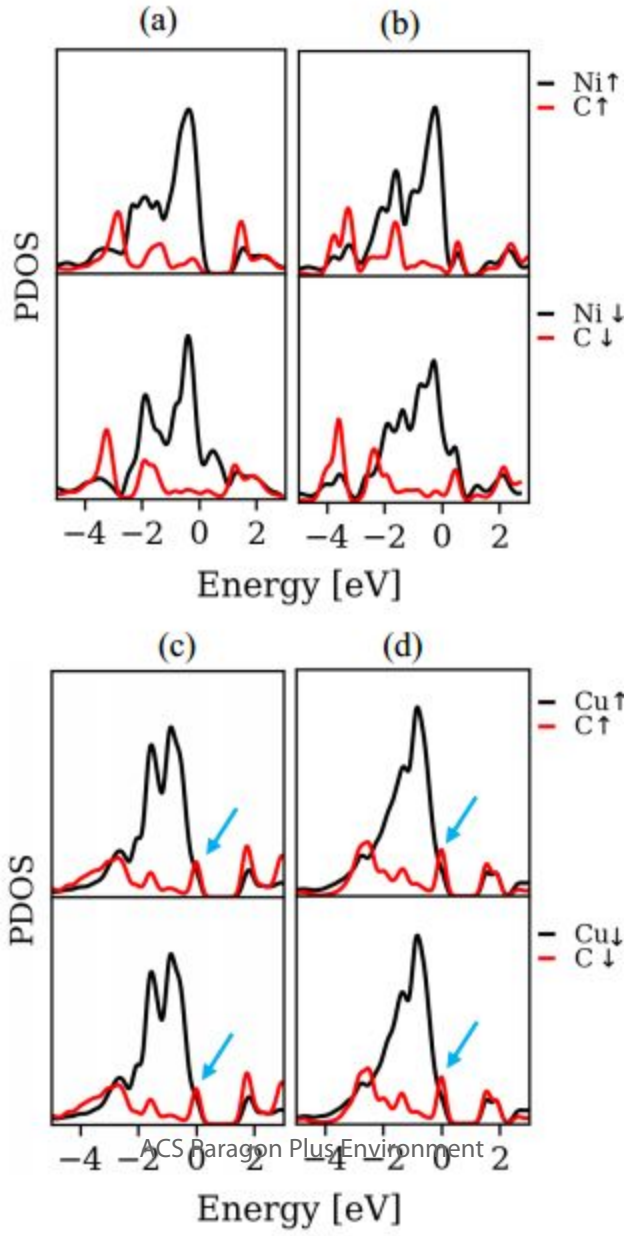

Figure 10: Projected density of states for the adsorption of CO_2 molecule on TiO_2 supported: a) Ni_5-neutral, b) Ni_5-charged, c) Cu_5-neutral, d) Cu_5-charged structures

Table 2: Bond lengths and adsorption energies of CO_2 molecules on TiO_2-supported Ni_5 and Cu_5 clusters

Method	Structure	r(C-O)	α (OCO)	E_{ads} (eV)
DFT	Gas Phase	1.17, 1.17	180	

	Ni_5-Neutral	1.22, 1.27	135.9	-0.53
	Ni_5-Charged	1.26, 1.32	124.2	-2.69
	Cu_5-Neutral	1.25, 1.28	131.0	-0.75
	Cu_5-Charged	1.25, 1.30	125.6	-1.57
DFT+U	Ni_5-Neutral	1.23, 1.27	134.3	-0.31
	Ni_5-Charged	1.26, 1.32	123.7	-2.53
	Cu_5-Neutral	1.25, 1.29	129.5	-0.64
	Cu_5-Charged	1.25, 1.29	125.8	-1.10

By looking into the bond lengths and angles reported in Table 2, we can see that the bond length elongation and bending of the O-C-O angle in the Ni_5 case is more sensitive to excess charge than in the Cu_5 case. This agrees with the more stable bent structure of the CO_2 adsorbed on supported Ni_5.

Dissociated CO_2 on TiO_2, Ni_5/TiO_2 and Cu_5/TiO_2

In plasma catalysis CO_2 dissociation can occur via several reaction paths. In this work, we focus on the adsorption of CO_2 on neutral and negatively charged surfaces, and not on the actual reaction paths. Hence, these simulations do not aim to identify the most suitable catalyst for CO_2 dissociation, but they provide more insight in the effect of surface charging, which is one of the characteristic features of plasma catalysis, distinguishing it from thermal catalysis. In order to estimate the effect of charge on the dissociation of CO_2, we examined various initial configurations of dissociated CO_2 (CO(ads) + O(ads)) on TiO_2, Ni_5/TiO_2 and Cu_5/TiO_2.

For CO_2 dissociation on neutral TiO_2, we did not find a stable structure for adsorbed CO(ads). In most cases, CO either desorbs back in the gas phase or attracts an oxygen atom from the surface and so forms a linear CO_2 molecule. We have provided a less stable structure in Fig. 11a, in which

the CO(ads) + O(ads) phase is achieved. Although results in Fig. 12 for dissociation on the bare surface of TiO_2 show an improvement in the adsorption energy due to the presence of the excess electron, dissociative adsorption is thermodynamically unfavorable, regardless of charging. This means that in the absence of a catalyst, dissociation of CO_2 on a bare slab of anatase will not proceed. An interesting parallel can be drawn with the effect of vacancies on the reactivity of TiO_2 towards CO_2 activation. Just like the formation of vacancies, electron addition effectively corresponds to a reduction of the TiO_2 surface. In both cases, this reduction has been found to result in an improved chemisorption of CO_2. However, vacancies additionally provide a strong binding site for oxygen[44, 47], thus also promoting the dissociation of CO_2 adsorbed on a vacancy; such site is not created upon charging, and CO_2 splitting remains unfavorable.

By employing Ni_5 as catalyst, we find a dissociative adsorption energy of -0.03 eV for the CO_2 dissociation on the neutral surface (Fig. 11c). By adding an excess electron to the system the adsorption energy significantly increases to -1.85 eV, which makes the reaction thermodynamically highly favorable (Fig. 11d).

For the case of neutral Cu_5/TiO_2, dissociation of the CO_2 molecule into adsorbed $(CO)_{ads}$ and $(O)_{ads}$ is slightly endothermic with an adsorption energy of $+0.14$ eV (Fig. 11e). Upon negatively charging the system, (Fig. 11f) the dissociative adsorption energy becomes -0.25 eV, making this reaction thermodynamically favourable. Fig. 12 shows the corresponding dissociative adsorption energy for each configuration based on DFT and DFT+U calculations.

These results show that the presence of an excess electron has a positive impact on stabilization of the dissociated CO_2. This impact is more pronounced in case of a Ni pentamer as catalyst, which shows excellent performance in response to the presence of a plasma-induced excess electron and significantly improves the adsorption energy of both adsorbed and dissociated CO_2. Cu_5 adsorbed

on a neutral TiO_2 surface is not active enough to dissociate the CO_2 in a favorable way, but it also shows positive feedback to negatively charging the surface. Therefore, these two particular test cases (adsorbed Ni_5 and Cu_5) are good examples of how electrons from a non-equilibrium plasma can induce a shift in the chemical properties of different catalysts.

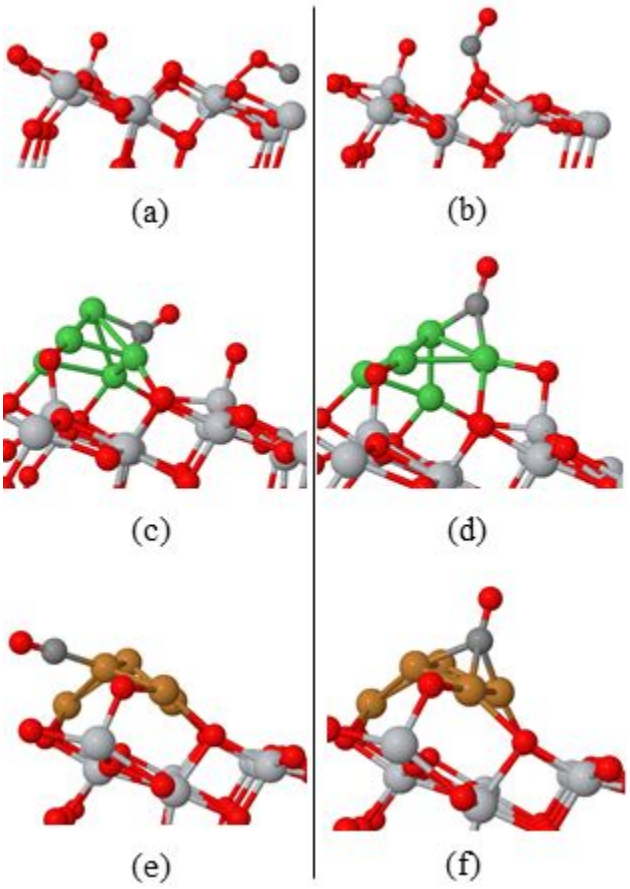

Figure 11: The most stable dissociated structures for CO_2 (CO(ads) + O(ads)) on a) neutral TiO_2, b) charged TiO_2, c) neutral Ni_5/TiO_2, d) charged Ni_5/TiO_2, e) neutral Cu_5/TiO_2 and f) charged Cu_5/TiO_2

While there are small differences in bond lengths and also adsorption energies in the results obtained from DFT and DFT+U, trends regarding the effect of charge on CO_2 activation are the same for both approaches. In addition to the comparison between the DFT and DFT+U results, we have also investigated the effect of change in surface charge density. We did the same calculations

for CO_2 adsorption on pristine titania by using a larger slab (2 × 4 supercell) of anatase TiO_2 (101) corresponding to a surface charge density of $-0.05 \frac{C}{m^2}$ which is 2.7 times less than the small slab. The results indicate that for the large slab, the trends in the effect of charge on stabilization of the bent CO_2 molecule remain the same, although less pronounced (see the SI).

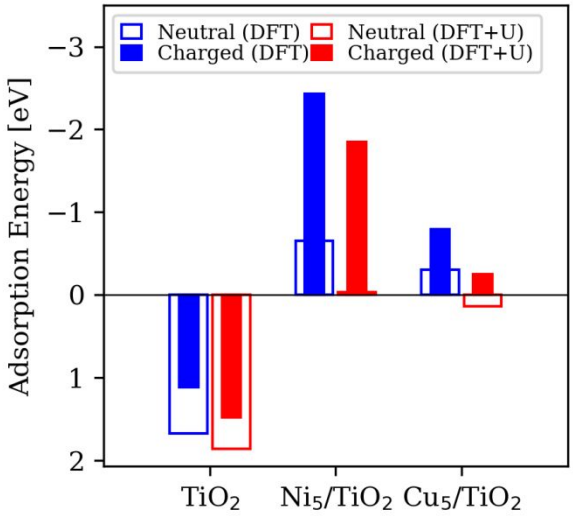

Figure 12: Dissociative adsorption energy of CO_2 on bare TiO_2, Ni_5/TiO_2 and Cu_5/TiO_2

Conclusion

In this study, we investigated the effect of excess electrons induced by plasma on the adsorption properties of Ni_5 and Cu_5 clusters over the anatase TiO_2 (101) surface and also CO_2 activation on both pristine a-TiO_2 and supported clusters.

Adsorption of Ni_5 and Cu_5 clusters on the surface of anatase (101) in the neutral case leads to a charge transfer between the cluster and the support. Depending on the type of catalyst, the direction of charge transfer can be from surface to the cluster and vice versa. In this case, negatively charging the system leads to minor changes in stabilization of the clusters. If the excess electron is localized on the surface, it will have a more pronounced impact than when the electron is localized on the

cluster. Negatively charging the surface for adsorption of the CO_2 on a bare slab of anatase (101) causes the most stable structure of the CO_2 molecule to change from a linear to a bent configuration. This is mostly because of shifting the high-lying CO_2 antibonding π^* orbitals towards the valence band and facilitating their hybridization with *p* or *d* states of the surface.

In the case of employing Cu_5 and Ni_5 nanoclusters, the same result is seen for the improvement of bent CO_2 stabilization, although the underlying mechanisms are slightly different. Upon negatively charging the system in CO_2 adsorption on supported Ni_5, the same shifting in CO_2 high-lying states is seen, which leads to increased hybridization with the cluster d orbitals. In contrast, for the supported Cu_5, changing the adsorption site from the interface to the cluster leads to more stabilization of the CO_2 molecule. This change in adsorption mode results in a significant increase in the negative partial charge of the CO_2 molecule, which can be considered as indicative for activation of the molecule[43].

The dissociation of CO_2 on a bare slab of anatase titania is thermodynamically unfavourable, regardless of added charge. CO_2 dissociation is favourable on Cu_5 as catalyst in a charged configuration, and on Ni_5 both in neutral and charged configurations. Together with better results for adsorption energy and bond elongation of the CO_2 (ads) in charged configurations, Ni_5 could be a good option for plasma catalysis aiming to CO_2 conversion.

In general, plasma-induced excess electrons alter the adsorption process, by shifting the anti-bonding states of CO_2 towards the valence band, increasing the polarization effects and changing the adsorption site of the molecule. These effects consequently lead to improved stabilization of bent (ads) and dissociated CO_2 in negatively charged structures. This can be considered as a possible reason for the synergistic effects in plasma catalysis.

Associated Content

The supporting information is available free of charge.

Isolated Ni_5 and Cu_5 clusters, unstable structures for the Ni_5 and Cu_5 cluster adsorption on TiO_2 surface, PDOS plots for adsorption of clusters on TiO_2 (101), results for structures with fixed bottom layers, calculations with (2×4) supercell of TiO_2 (101) (constrained and fully relaxed structures) and tables of spin moments and net charges.

Author information

Corresponding author

Email: amin.jafarzadeh@uantwerpen.be

Tell: +32-32652360

Fax: +32-32652343

Acknowledgment

The authors acknowledge financial support from the TOP research project of the Research Fund of the University of Antwerp (grant ID: 32249). K.M.B. was funded as PhD fellow (aspirant) of the FWO-Flanders (Research Foundation - Flanders), Grant 11V8915N. The computational resources and services used in this work were provided by the VSC (Flemish Supercomputer Center), funded by the FWO and the Flemish Government – department EWI.

References

[1] Neyts, E. C. and Bogaerts, A. Understanding plasma catalysis through modelling and simulation-A review, *J. Phys. D: Appl. Phys.* **2014,** 47,224010

[2] Neyts, E. C.; Ostrikov, K. (K.); Sunkara, M. K. and Bogaerts, A. Plasma Catalysis: Synergistic Effects at the Nanoscale, *Chem. Rev.* **2015,** 115, 13408-13446

[3] Kim, H.-H.; Ogata, A.; Schiorlin, M.; Marotta, E. and Paradisi, C. Oxygen Isotope (18O2) Evidence on the Role of Oxygen in the Plasma-Driven Catalysis of VOC Oxidation, *Catal. Lett.* **2011,** 141, 277-282

[4] Maciuca, A.; Batiot-Dupeyrat, C. and Tatibouet, J.-M. Synergetic effect by coupling photocatalysis with plasma for low VOCs concentration removal from air, *Appl. Catal., B* **2012,** 125, 432 - 438

[5] Jogi, Indrek; Erme, Kalev; Haljaste, Ants and Laan, Matti Oxidation of nitrogen oxide in hybrid plasma-catalytic reactors based on DBD and Fe2O3* *Eur. Phys. J. Appl. Phys.* **2013,** 61, 24305

[6] Mizuno, A. Generation of non-thermal plasma combined with catalysts and their application in environmental technology, *Catal. Today* **2013,** 211, 2 - 8

[7] Tatarova, E.; Bundaleska, N.; Sarrette, J. P. and Ferreira, C. M. Plasmas for environmental issues: from hydrogen production to 2D materials assembly, *Plasma Sources Sci. Technol.* **2014,** 23, 063002

[8] Kim, H.-H.; Teramoto, Y.; Ogata, A.; Takagi, H. and Nanba, T. Plasma Catalysis for Environmental Treatment and Energy Applications, *Plasma Chem. Plasma Process.* **2016,** 36, 45-72

[9] Lee, H. and Sekiguchi, H. Plasma-catalytic hybrid system using spouted bed with a gliding arc discharge: CH_4 reforming as a model reaction, *J. Phys. D: Appl. Phys.* **2011,** 44, 274008

[10] Tu, X.; Gallon, H. J.; Twigg, M. V.; Gorry, P. A. and Whitehead, J. C. Dry reforming of methane over a Ni/Al_2O_3 catalyst in a coaxial dielectric barrier discharge reactor, *J. Phys. D: Appl. Phys.* **2011,** 44, 274007

[11] Zhang, L.; ling Sha, X.; Zhang, L.; bin He, H.; hua Ma, Z.; wei Wang, L.; xin Wang, Y. and xia She, L. Synergistic catalytic removal NOX and the mechanism of plasma and hydrocarbon gas, AIP Advances **2016,** 6, 075015

[12] Mei, D.; Yan, J. and Tu, X. Plasma-catalytic conversion of CO_2 into value-added chemicals: Understanding the synergistic effect at low temperatures, **2015**, 1-1. DOI: 10.1109/PLASMA.2015.7179620

[13] Kim, J.; Go, D. B. and Hicks, J. C. Synergistic effects of plasma-catalyst interactions for CH_4 activation, *Phys. Chem. Chem. Phys.* **2017,** 19, 13010-13021

[14] Zhou, R.; Zhou, R.; Zhang, X.; Li, J.; Wang, X.; Chen, Q.; Yang, S.; Chen, Z.; Bazaka, K. and (Ken) Ostrikov, K. Synergistic Effect of Atmospheric-pressure Plasma and TiO_2 Photocatalysis on Inactivation of Escherichia coli Cells in Aqueous Media, *Sci. Rep.* **2016**, 6

[15] Nørskov, J. Electronic factors in catalysis, *Prog. Surf. Sci.* **1991**, 38, 103 - 144

[16] Holzer, F.; Roland, U. and Kopinke, F.-D. Combination of non-thermal plasma and heterogeneous catalysis for oxidation of volatile organic compounds: Part 1. Accessibility of the intra-particle volume, *Appl. Catal., B* **2002**, 38, 163 - 181

[17] Durme, J. V.; Dewulf, J.; Sysmans, W.; Leys, C. and Langenhove, H. V. Efficient toluene abatement in indoor air by a plasma catalytic hybrid system, *Appl. Catal., B* **2007**, 74, 161 - 169

[18] Shirazi, M.; Bogaerts, A. and Neyts, E. C. A DFT study of H-dissolution into the bulk of a crystalline Ni(111) surface: a chemical identifier for the reaction kinetics, *Phys. Chem. Chem. Phys.* **2017**, 19, 19150-19158

[19] Shirazi, M.; Neyts, E. C. and Bogaerts, A. DFT study of Ni-catalyzed plasma dry reforming of methane, *Appl. Catal. B* **2017**, 205, 605 - 614

[20] Chen, H.-Y. T.; Tosoni, S. and Pacchioni, G. Adsorption of Ruthenium Atoms and Clusters on Anatase TiO_2 and Tetragonal ZrO_2(101) Surfaces: A Comparative DFT Study, *J. Phys. Chem. C* **2015**, 119, 10856-10868

[21] Puigdollers, A. R.; Schlexer, P. and Pacchioni, G. Gold and Silver Clusters on TiO_2 and ZrO_2 (101) Surfaces: Role of Dispersion Forces, *J. Phys. Chem. C* **2015**, 119, 15381-15389

[22] Tosoni, S.; Chen, H.-Y. T. and Pacchioni, G. A DFT study of Ni clusters deposition on titania and zirconia (101) surfaces, *Surf. Sci.* **2016**, 646, 230 - 238

[23] Liu, C.; Yang, B.; Tyo, E.; Seifert, S.; DeBartolo, J.; von Issendorff, B.; Zapol, P.; Vajda, S. and Curtiss, L. A. Carbon Dioxide Conversion to Methanol over Size-Selected Cu_4 Clusters at Low Pressures, *J. Am. Chem. Soc.* **2015**, 137, 8676-8679

[24] Fuzhen, Z.; Miao, G.; Kun, C.; Yuhua, Z.; Jinlin, L. and Rong, C. Atomic Layer Deposition of Ni on Cu Nanoparticles for Methanol Synthesis from CO_2 Hydrogenation, *ChemCatChem* **2017**, 9, 3772-3778

[25] Diebold, U.; Ruzycki, N.; Herman, G. and Selloni, A. One step towards bridging the materials gap: surface studies of TiO_2 anatase, *Catal. Today* **2003**, 85, 93-100

[26] Li, Y.-F. and Selloni, A. Theoretical Study of Interfacial Electron Transfer from Reduced Anatase TiO_2(101) to Adsorbed O_2, *J. Am. Chem. Soc.* **2013**, 135, 9195-9199

[27] VandeVondele, J.; Krack, M.; Mohamed, F.; Parrinello, M.; Chassaing, T. and Hutter, J. Quickstep: Fast and accurate density functional calculations using a mixed Gaussian and plane waves approach, *Comput. Phys. Commun.* **2005**, 167, 103 - 128

[28] Hutter, J.; Iannuzzi, M.; Schiffmann, F. and VandeVondele, J. cp2k: atomistic simulations of condensed matter systems, *Wiley Interdiscip. Rev.: Comput. Mol. Sci.* **2013**, 4, 15-25

[29] VandeVondele, J. and Hutter, J. Gaussian basis sets for accurate calculations on molecular systems in gas and condensed phases, *J. Chem. Phys.* **2007**, 127, 114105

[30] Goedecker, S.; Teter, M. and Hutter, J. Separable dual-space Gaussian pseudopotentials, *Phys. Rev. B* **1996**, 54, 1703-1710

[31] Krack, M. Pseudopotentials for H to Kr optimized for gradient-corrected exchange-correlation functionals, *Theor. Chem. Acc.* **2005**, 114, 145-152

[32] Perdew, J. P.; Burke, K. and Ernzerhof, M. Generalized Gradient Approximation Made Simple, *Phys. Rev. Lett.* **1996**, 77, 3865-3868

[33] Grimme, S.; Antony, J.; Ehrlich, S. and Krieg, H. A consistent and accurate ab initio parametrization of density functional dispersion correction (DFT-D) for the 94 elements H-Pu, *J. Chem. Phys.* **2010**, 132, 154104

[34] Grimme, S.; Ehrlich, S. and Goerigk, L. Effect of the damping function in dispersion corrected density functional theory, *J. Comput. Chem.* **2011**, 32, 1456-1465

[35] Bultinck, P.; Alsenoy, C. V.; Ayers, P. W. and Carbo-Dorca, R. Critical analysis and extension of the Hirshfeld atoms in molecules, *J. Chem. Phys.* **2007**, 126, 144111

[36] Howard, C. J.; Sabine, T. M. and Dickson, F. Structural and thermal parameters for rutile and anatase, *Acta Crystallogr., Sect. B: Struct. Sci.* B **1991**, 4, 462-468

[37] Bal, K. M.; Huygh, S.; Bogaerts, A. and Neyts, E. C. Effect of plasma-induced surface charging on catalytic processes: application to CO_2 activation, *Plasma Sources Sci. Technol.* **2018,** 27, 024001

[38] Martyna, G. J. and Tuckerman, M. E. A reciprocal space based method for treating long range interactions in ab initio and force-field-based calculations in clusters, *J. Chem. Phys.* **1999**, 110, 2810-2821

[39] Bal, K. M.; Neyts, E. C. Modelling Molecular Adsorption on Charged or Polarized Surfaces: a Critical Flaw in Common Approaches. *Phys. Chem. Chem. Phys.* **2018**, *20*, 8456–8459.

[40] Anisimov, V. I.; Zaanen, J. and Andersen, O. K. Band theory and Mott insulators: Hubbard U instead of Stoner I, *Phys. Rev. B* **1991,** 44, 943-954

[41] Dudarev, S. L.; Botton, G. A.; Savrasov, S. Y.; Humphreys, C. J. and Sutton, A. P. Electron-energy-loss spectra and the structural stability of nickel oxide: An LSDA+U study, *Phys. Rev. B* **1998**, 57, 1505-1509

[42] Hahn, K. R.; Seitsonen, A. P.; Iannuzzi, M. and Hutter, Jü. Functionalization of CeO_2(111) by Deposition of Small Ni Clusters: Effects on CO_2 Adsorption and O Vacancy Formation, *ChemCatChem* **2015**, 7, 625-634

[43] Iyemperumal, S. K. and Deskins, N. A. Activation of CO_2 by supported Cu clusters, *Phys. Chem. Chem. Phys.* **2017**, 19, 28788-28807

[44] Sorescu, D. C.; Al-Saidi, W. A. and Jordan, K. D. CO_2 adsorption on TiO_2(101) anatase: A dispersion-corrected density functional theory study, *J. Chem. Phys.* **2011**, 135, 124701

[45] Zhang, Q.-Z.; Wang, W.-Z. and Bogaerts, A. Importance of surface charging during plasma streamer propagation in catalyst pores, *Plasma Sources Sci. Technol.* **2018**, 27, 065009

[46] Deskins, N. A.; Liu, C.; Iyemperumal, S. K.; Li, G. Photocatalytic CO_2 reduction by highly dispersed Cu sites on TiO_2, *J. Photonics Energy* **2016**, 7, 7 - 7 – 10

[47] Huygh, S.; Bogaerts, A. and Neyts, E. C. How Oxygen Vacancies Activate CO_2 Dissociation on TiO_2 Anatase (001), *J. Phys. Chem. C* **2016**, 120, 21659-21669

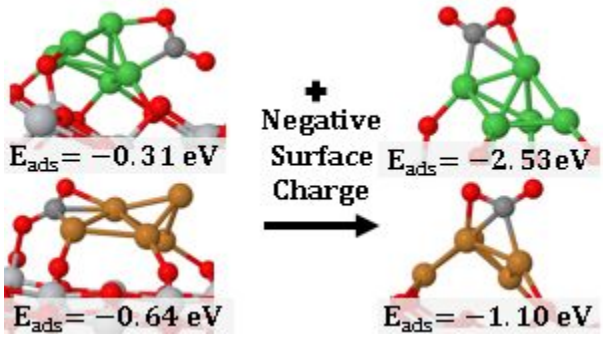

TOC Graphic

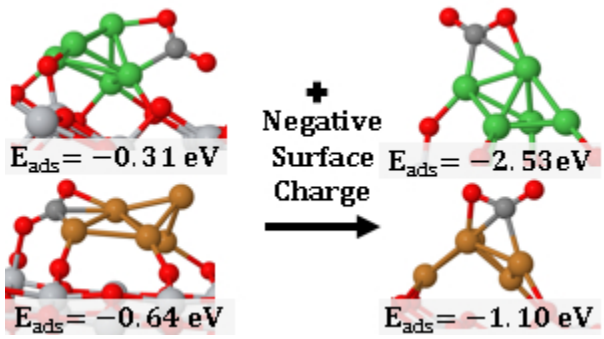

TOC

79x44mm (96 x 96 DPI)